A Deep Learning Study on Osteosarcoma Detection from Histological Images and Visualize the Neurons Activations

Rasel Mahmud (id: 20-43867-2)[1],**Sajjad Hossain Shakib** (id: *20-43842-2*)[2],
Md. Nafiul Islam Nayeem (id:*20-43678-2*)[3], **Md. Farhan Ul Asif**
(id: *20-43522-1*)[4]

[a]*Department of Computer Sciences, American International University-Bangladesh*

Abstract

In this Study, a Comprehensive deep-learning investigation was conducted for Osteosarcoma detection from histological images. Osteosarcoma is a malignant bone cancer, that poses significant challenges in the diagnosis due to its complex patterns and variations in nature. A previous Study proposed that modified VGG19 Architecture shows significantly better results in Osteosarcoma detection in histological images for Osteosarcoma detection. The Study employed advanced techniques to visualize the activations of neurons in the VGG19 model. These visualizations reveal the model's inner workings by showing how particular characteristics and patterns in the histological pictures affect the behavior of individual neurons. Researchers could better grasp the decision-making process of the model by learning which areas of the input images each neuron was sensitive to using activation visualization. The results of the study showed how well the deep learning model was able to identify osteosarcoma from histology images reliably. Additionally, the neuron activation visualizations provided a bridge between the technical components of deep learning and the interpretability of its outcomes, providing a qualitative interpretation of the model's acquired representations.

Keywords: ***Deep learning, Computer Vision, Bone Cancer, Histological Image, Object detection, NN, CNN***

1. INTRODUCTION

Osteosarcoma is the predominant form of cancer commonly observed among adolescents, originating in the bones, typically in the arms or legs. The average age of identification for osteosarcoma is 15, and it predominantly impacts teenagers More than 75 percent of the cases are represented by individuals under the age of 25 [1]. Annually, the United States witnesses around 400 to 1,000 fresh instances of osteosarcoma. Following brain tumors and lymphomas, osteosarcoma ranks as the third most prevalent cancer among adolescents [2]. The exact root cause of osteosarcoma remains uncertain. Nevertheless, various factors increase the risk, such as rapid bone growth, exposure to radiation, genetic predisposition, and bone fractures. Common indications of osteosarcoma encompass bone pain, a palpable

warm lump on the skin, inflammation at the tumor location, and escalating unease upon movement [3]. The essential methods for diagnosing osteosarcoma encompass MRI, X-ray, computed tomography (CT), biopsy, bone scans, and PET scans [4]. X-rays are employed to identify abnormal bone growths. MRI employs a strong magnet, radio waves, and a computer to generate detailed images of bodily structures. CT employs multiple X-ray images to create cross-sectional views of internal body processes using computer technology. Biopsy entails extracting a tissue sample from the affected region to analyze cancer cells. For bone-related diagnoses, a small quantity of radioactive material is introduced into the body [5]. The National Cancer Institute (NCI) emphasizes the importance of improving diagnostic precision and identifies misdiagnosis and delayed diagnoses as persistent challenges. Histopathological examination stands as a vital element in cancer diagnosis, demanding specialized expertise that might not be universally accessible. To address these challenges, the potential of employing advanced techniques like deep learning to augment diagnostic capabilities is being explored [8]. Considering this background, our primary objective is to significantly propel the field of cancer diagnosis, particularly concentrating on osteosarcoma. We aim to develop a dependable and accurate system capable of analyzing histological images from bone cell samples, identifying potential osteosarcoma tumors through the capabilities of deep learning algorithms, and comprehending neuronal activation within the model. This research endeavors to bridge the divide between existing diagnostic methods and the growing potential of AI-driven treatments [9].

As histological images are complex in nature and previous study shows that VGG19 model shows a significant results in the Bone Cancer detection out aim is to visualize the behaviors of the neurons as well as the Filters in the Convolutional layers. Using a publicly available dataset, the project demonstrating Deep Learning capabilities for osteosarcoma malignancy detection intends to demonstrate the potential of Deep Learning technologies for properly identifying osteosarcoma malignancy. Investigating an appropriate deep learning framework that enables accurate tumor malignancy diagnosis and, in the process, identifies key elements enhancing model performance is the goal of exploring optimal deep learning framework and performance indicators. The study investigating performance enhancement through Model Generalization investigates the capacity of the generated deep learning models to generalize well across multiple dataset types.

1.What effect do various pre-processing techniques have on how well deep learning models for osteosarcoma detection perform?

Using histology images, the study is likely focused on the application of deep learning techniques to enhance osteosarcoma identification and diagnosis [11]. Histological images, which are microscopic images of tissue samples, are very important in the diagnosis of several diseases, including cancer. This study shows the effectiveness of deep learning for osteosarcoma identification in medical image analysis, the advantages of transfer learning with VGG19 model as input for increased accuracy. The findings might improve the discipline of histological image analysis and help in better osteosarcoma diagnosis.

2. LITERATURE REVIEW

Medical image analysis has seen a revolution in recent years thanks to the use of computer-

aided technologies, specifically deep convolutional neural networks (CNNs) [12]. A few disorders, including breast cancer, pulmonary edema, pneumonia, gastric ailments, and gastric cancer, have been detected because of this technical innovation [13][14]. When it comes to conditions like osteosarcoma, where early detection can have a substantial impact on patient outcomes, the potential for early diagnosis by autonomous systems is very important.

The use of CNNs becomes extremely pertinent in the framework of histological image analysis, where the goal is to identify tissue morphological changes. Like many other diseases, osteosarcoma has specific tissue patterns that can be easily identified through image analysis. Early detection of these patterns may be essential for reducing the risk of metastasis and enhancing patient outcomes. CNNs can not only decrease the possibility of misdiagnosis but also help surgeons identify metastases, thereby reducing their burden and improving patient care.

Although most deep learning studies in histological image analysis have been directed at breast cancer, there is evidence that these techniques can also be applied to osteosarcoma. Studies on the histology of breast cancer have shown the value of transfer learning, with trained models like VGG16 and AlexNet achieving outstanding levels of accuracy [17]. These findings show that these models are appropriate for the classification of images and imply that osteosarcoma detection can benefit from similar methodologies.

Other examples of image classification in recent years use similar methods: Jonathan De Matos [15] used double transfer learning to classify histopathologic images. Noorul Wahab [20] aimed at a more challenging task of segmentation and detection of mitotic nuclei. They used a similar hybrid CNN model and achieved a 76% AUC value. Other examples include the prediction of pathological invasiveness in lung adenocarcinoma [21], Classification of Liver Cancer Histopathology Images [19], and Automated invasive ductal carcinoma detection [22].

A fully automated approach for evaluating viable and necrotic tumors in osteosarcoma using histology pictures and deep-learning models was introduced in one particularly important study [16] by Harish Babu Arunachalam. This study set out to categorize various tissue locations into groups for viable tumors, necrotic tumors, and non-tumor regions. With class-specific accuracy levels of 91.9% for non-tumors, 95.3% for viable tumors, and 92.7% for necrotic tumors, the collective learning model obtained a remarkable overall accuracy of 93.3%.

The idea of information transfer is important for the effectiveness of deep learning models in medical image processing. Pre-trained networks used for larger datasets from similar areas can provide important parameters for effectively training deep learning models when labeled training data has limitations inside a particular study domain. This information transfer strategy has been demonstrated to greatly increase learning results while requiring less time and effort to classify large amounts of data [18].

In the domain of histological image analysis, recent developments in deep learning and CNNs have demonstrated important commitment, with applications extending above osteosarcoma diagnosis. To achieve high levels of accuracy in identifying tissue patterns, transfer learning and the use of pre-trained models have become important. The result has opened the way for more dependable and effective diagnostic tools in the battle against

osteosarcoma.

3. PROPOSED METHOD

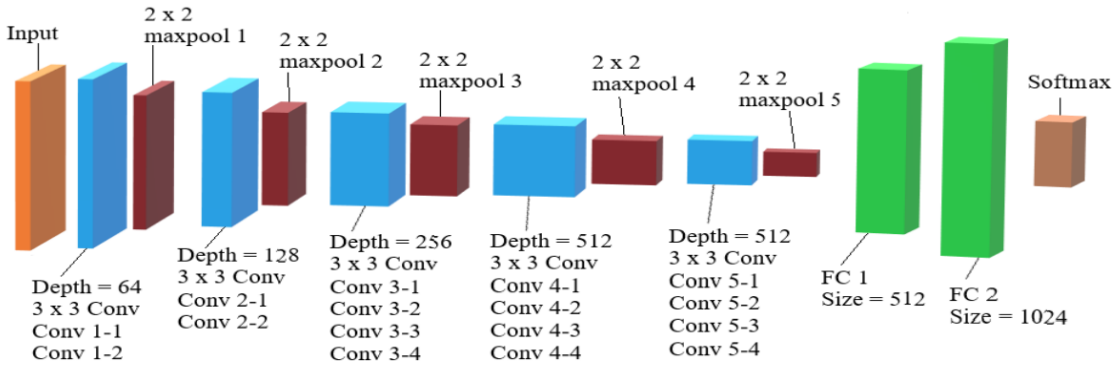

Figure 1: VGG19 Network Architecture for Multiclass Classification

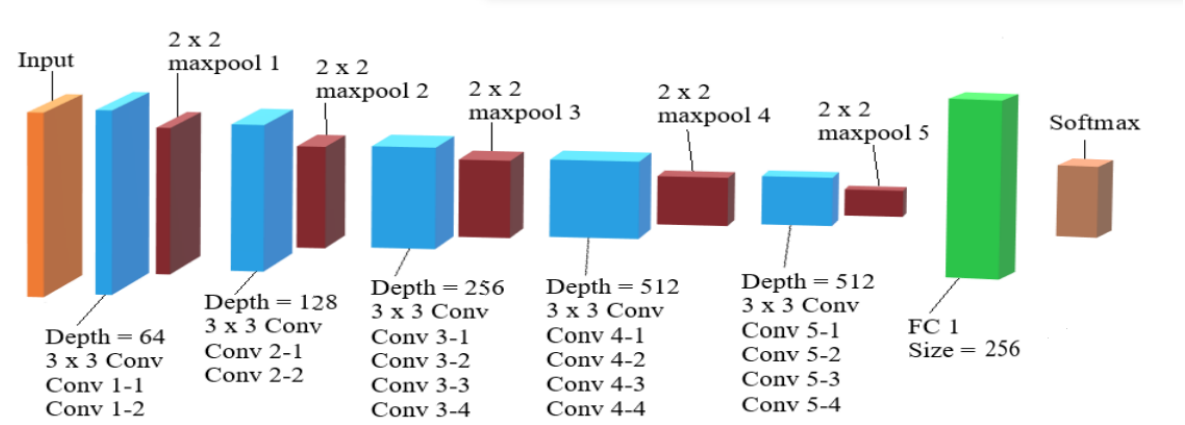

Figure 2: Modified VGG19 Architecture for Binary Classification

In our Proposed Method We have used Modified VGG19 Proposed by (Anisuzzaman et al.) Architecture for Multiclass Classification and another modified VGG19 Architecture for Binary Classification. We have taken the Dataset from (Anisuzzaman et al.). There are 1144 images of Different Bone Cancer conditions in Histological images. In Multiclass Classification total of 800 images are used for training the model, 274 images are used for validation and the remaining images are used for testing the model performance. 1500 epochs are done for Multiclass classification and all the images are 375x375 dimension. The batch size for model training and validation is 28 and 16 in multiclass classification. In Multiclass classification no data Augmentation we performed. In Binary classification, the

classification was performed in Non-Tumor vs. Viable Tumor, Non-Tumor vs. Non-Viable-Tumor and Non-Viable-Tumor vs. Viable Tumor. In binary classification total of 100 epochs are performed in each Binary Classification and Data Augmentation was also performed to increase the variability in the dataset during the training of the model.

4. RESULTS

In Multiclass classification the Accuracy was gained 88.57% in the model proposed by (Anisuzzaman et al.). And in Binary classification, our modified model gained 98% accuracy in the test dataset for the 'Non-Tumor' vs 'Viable' classification, 96.15% accuracy in the test dataset for the 'Non-Tumor' vs "Non-Viable-Tumor' classification, 91.89% accuracy in the test dataset for ' Viable ' vs "Non-Viable-Tumor'. The Models provides significant results in the histological dataset and VGG19 provides better results compared to other model due to its structure. Due to the use of a pre-trained model in a large number of datasets (imagenet), the model is already pre-trained on a large amount of data.

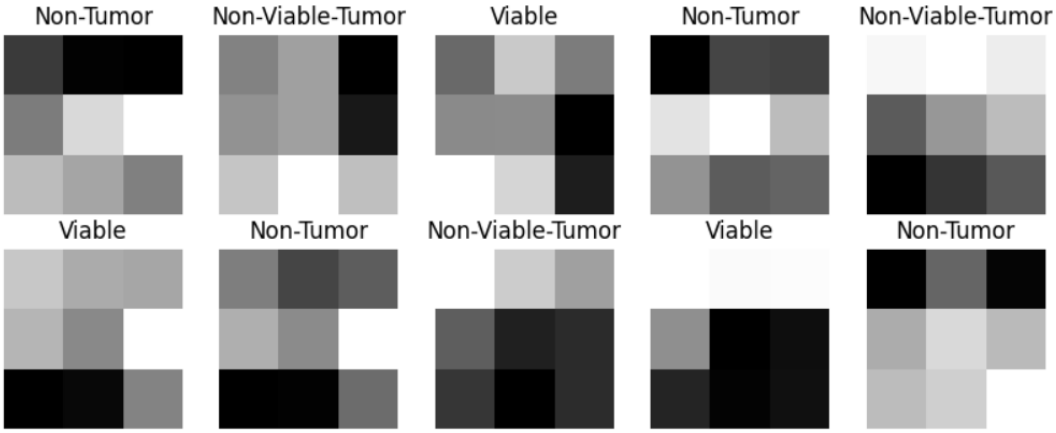

Fig: 3(Multiclass Filter Extraction in block5_conv4 a small portion of all filter)

Fig: 2 shows some of the Filter feature extraction region. In VGG19 model the filter are in uniform size 2x2 and which gives it advantages to extract more meaning full features for the classification tasks. Fig:1 shows the filter extraction technique in block5_conv4 layer which is a convolutional layer. Here the white box represents a region of high activation or feature presence. The white-marked box actually contains the main significant feature that has been extracted from the dataset. The black marked boxes represent they contain the less significant features in the images and the filter doesn't respond significantly in this region of the dataset images and these areas are the low texture region. Gray regions represent areas where the filter detected some level of information, but it may not be a strong or distinctive feature. Light gray regions indicate areas where the filter responded more strongly to certain features or patterns in the input data. These regions might correspond to edges or textures that the filter is designed to detect. The most significant area in the image region is marked by the white box and the less significant area in the image region is marked by the black box by the filter. Figure 1 shows the feature extraction regions for

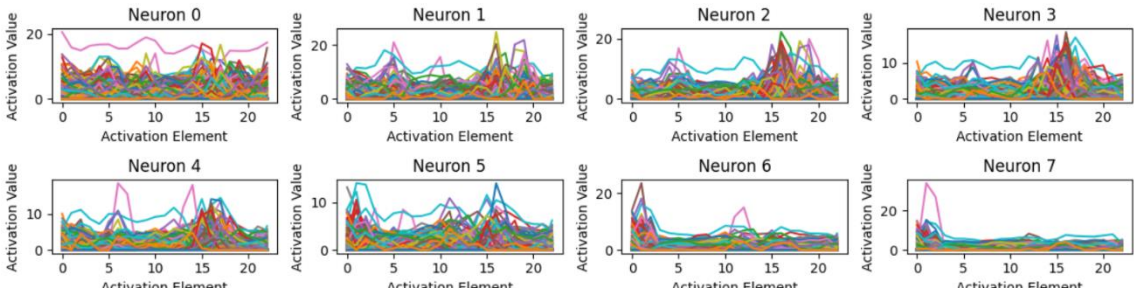

different class images in the dataset. For the small kernel size the kernel actually extract the more meaningful results and it's the reason why VGG19 performs better results in histological images as the images are complex in nature.

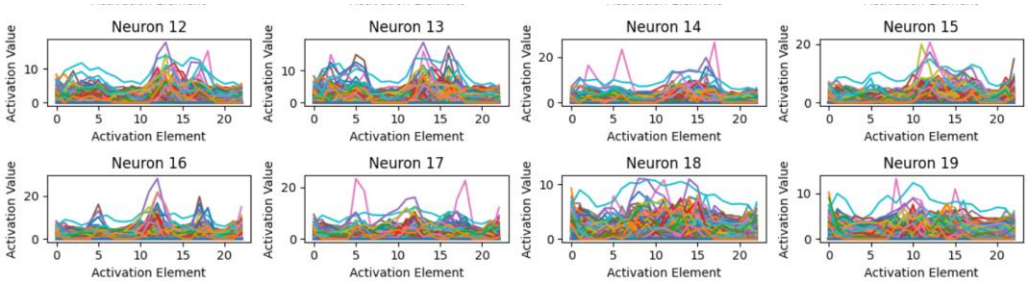

Fig: First Fully Connected Layer Neurons Activation for three different class(Multiclass Classification) a small portion of all neurons

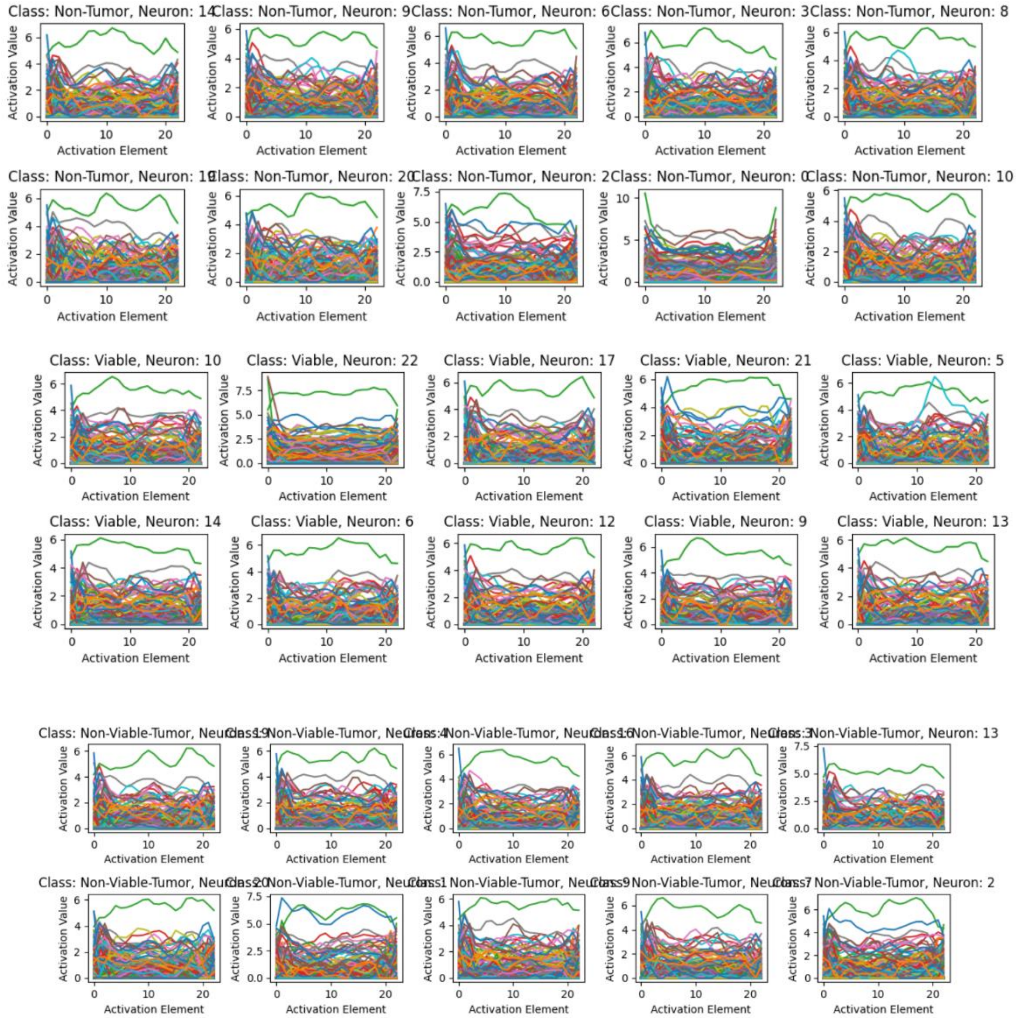

Fig: Last Fully Connected Layer Neurons Activation for three different class a small portion of all neurons

A neuron activation plot illustrates how individual neurons in a neural network layer react to specific patterns or traits within input data. Both the final and initial layer plots in multiclass classification visually represent the alteration in activation values for each neuron as they traverse different positions in the activation vector. These plots showcase the responsiveness of a subset of neuron to various input patterns or characteristics. Neurons with elevated activation values at specific positions exhibit heightened sensitivity to the patterns existing in the input data. Notable spikes or peaks in the plot can signify a neuron's identification of distinct features or patterns. The precise locations of these peaks correspond to points within the activation vector where the neuron's activation value is notably elevated. Diversity is apparent among neuron activation plots across different layers of the network. The more superficial layers tend to capture fundamental features, while deeper layers tend to engage with more intricate and sophisticated features. This plot indicates that these neurons effectively extract intricate and valuable features crucial for successful classification tasks.

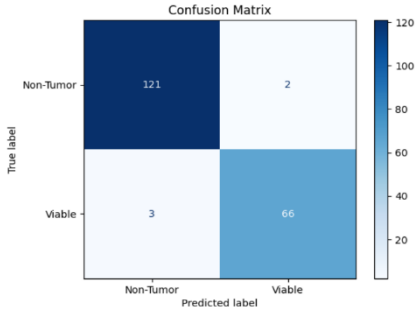

Fig: Confusion Matrix of the Binary Classification **'Non-Tumor', 'Viable'**

The performance of the binary classification model for distinguishing between 'Non-Tumor' and 'Viable' classes, as indicated by the confusion matrix, is highly impressive.

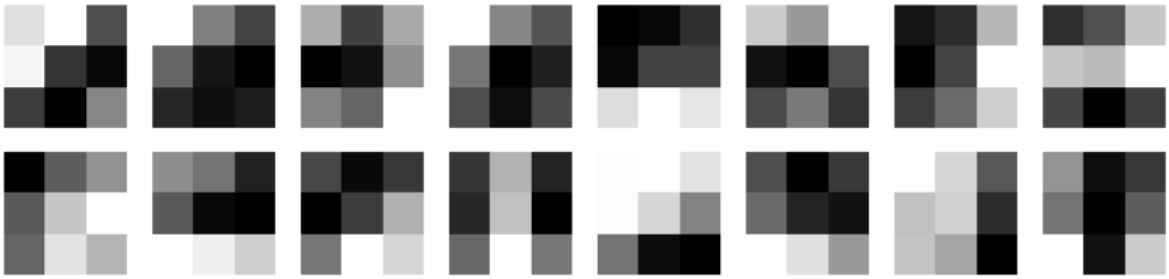

Fig:4(Binary Classification of 'Non-Tumor', 'Viable' Filter Extraction in block1_conv2) a small portion

The filters in the 2nd Convolutional layer highlight the regions that the filter deems important for feature extraction. Within the filter visualization, the white regions correspond to the most crucial areas in the images that contribute significantly to the classification process. Conversely, the darker regions represent areas that the kernel considers less significant for extracting relevant features.

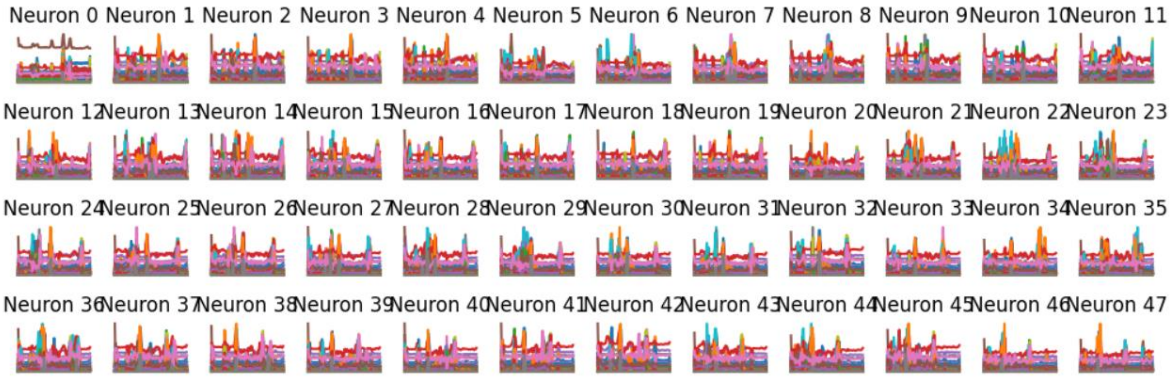

Fig: Fully Connected Layer Neurons Activation for binary classification('Non-Tumor', 'Viable')

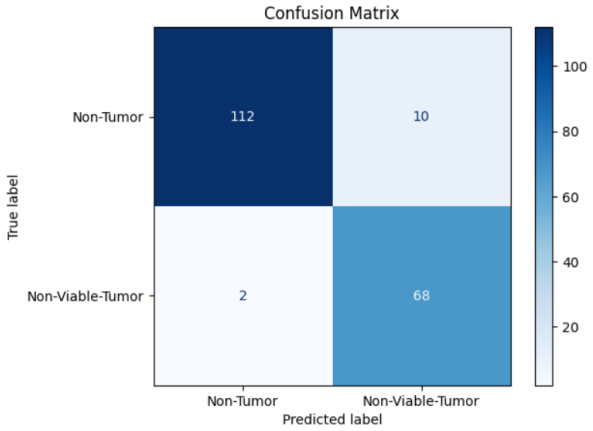

Fig: Confusion Matrix of the Binary Classification 'Non-Tumor', 'Non-Viable Tumor '

The performance of the binary classification model for distinguishing between 'Non-Tumor' and 'Non-Viable-Tumor' classes, as indicated by the confusion matrix, is highly impressive.

Fig:5(Binary Classification of 'Non-Tumor', 'Viable' Filter Extraction in block5_conv4) a small portion

The final filter before the Flatten operation in VGG19 plays a crucial role in identifying significant features within images. The filter highlights various regions in the image, designating white boxes for the most critical areas and darker regions for less important portions. This filter's activation aids in extracting key features for subsequent processing in the network.

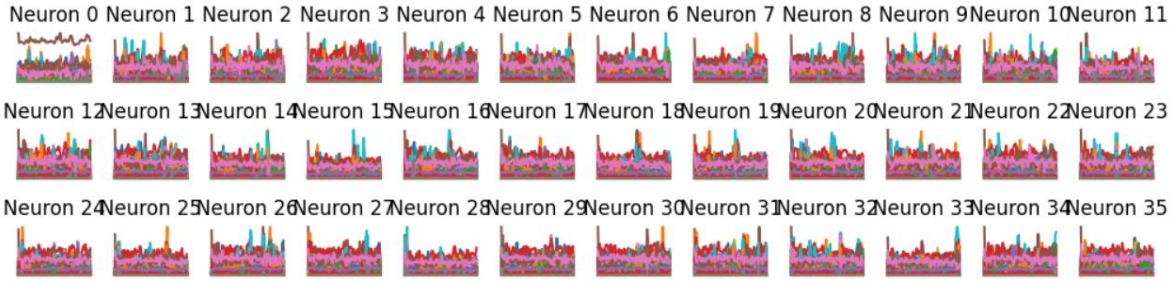

Fig: Fully Connected Layer Neurons Activation for binary classification('Non-Tumor', 'Viable') a small portion.

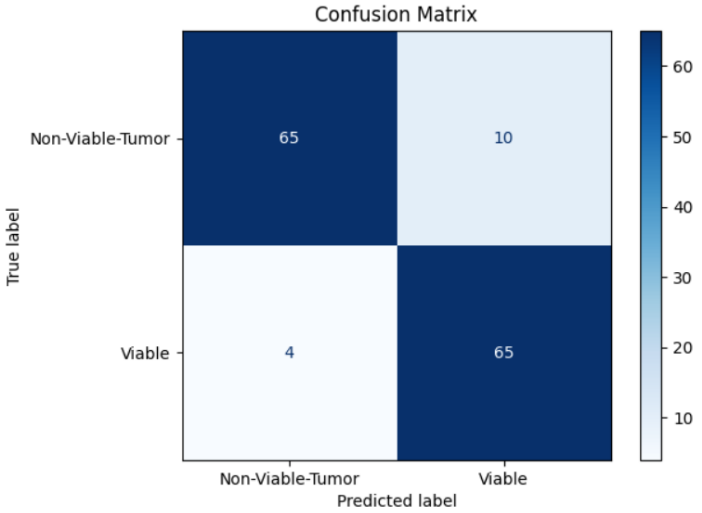

Fig: Confusion Matrix of the Binary Classification ‘Non- Viable -Tumor', 'Viable'

The performance of the binary classification model for distinguishing between 'Non-Viable-Tumor' and 'Viable' classes, as indicated by the confusion matrix, is highly impressive.

Fig:6(Binary Classification of ‘Non-Viable-Tumor', 'Viable' Filter Extraction in block5_conv4)

The ultimate filter preceding the Flatten operation within the VGG19 architecture assumes a pivotal role in pinpointing salient features within images. This filter effectively emphasizes different sections of the image, assigning white boxes to signify paramount regions and darker segments to denote less pivotal areas. The activation of this filter proves instrumental in the extraction of pivotal features, laying the groundwork for subsequent processing steps within the network.

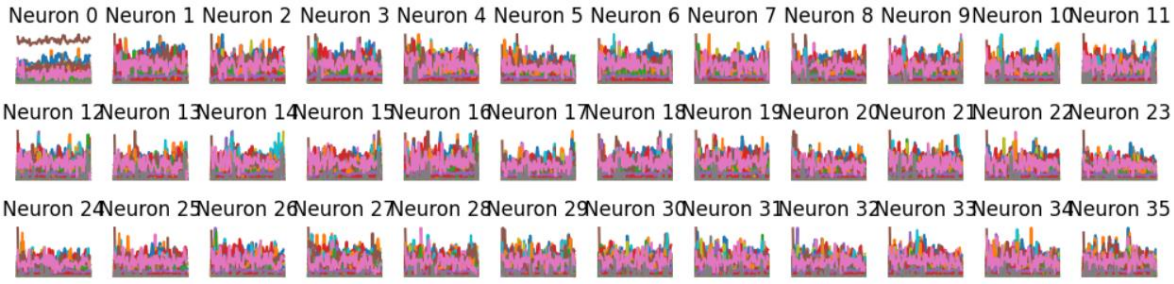

Fig: Fully Connected Layer Neurons Activation for binary classification('Non- Viable-Tumor', 'Viable')

In all the Fully Connected Layer Neurons Activation plot for binary classification The X-axis of the neuron activation plot corresponds to the position of individual neurons within the layer. Each neuron's activation is situated at a specific point along this axis. Meanwhile, the Y-axis reflects the activation value of a neuron at a particular position on the X-axis. This value represents the vigor or intensity of the neuron's response to the input data.

Elevated activation levels in a neuron signify a robust response to specific features or patterns present in the input data. Particularly in the realm of histological images for cancer

detection, heightened activation values often denote that the neuron has recognized noteworthy and pertinent attributes linked to cancerous or non-cancerous regions in the images. These attributes might encompass unique structures, textures, or other distinctive traits indicative of cancer presence or absence.

The observation that the majority of neurons in the activation plot exhibit higher activation values is indicative of their effective functionality. This phenomenon implies that these neurons are proficiently identifying pertinent features, contributing to more accurate outcomes. In essence, this outcome enhances the model's capacity to provide reliable and precise results in discerning between cancerous and non-cancerous areas within the histological images.

5.DISCUSSION

We delve into a comprehensive discussion of our deep-learning study focused on osteosarcoma detection using histological images. Our investigation encompassed multiclass classification, binary classifications, and the visualization of neuron activations, each offering valuable insights into the effectiveness and interpretability of our approach. Our study yielded a noteworthy multiclass classification accuracy of 88.57%, signifying the model's ability to accurately categorize histological images of varying osteosarcoma conditions. The binary classifications further showcased the model's robustness. Specifically, the model achieved an impressive accuracy of 98% in the 'Non-Tumor' vs 'Viable' classification, 96.15% accuracy in the 'Non-Tumor' vs 'Non-Viable-Tumor' classification, and 91.89% accuracy in the 'Viable' vs 'Non-Viable-Tumor' classification. These outcomes underscore the efficacy of our approach in distinguishing critical classes with a high level of accuracy. One of the highlights of our study was the visualization of neuron activations, particularly in the final convolutional layer. This visualization provided an insightful depiction of how the neural network processes information within the context of osteosarcoma detection. The visualization of kernels showcased regions of significance, where lighter areas indicated essential image components and darker regions represented less pivotal portions. This visualization contributes to the interpretability of the model's decision-making process and enhances our understanding of its internal mechanisms.

6.CONCLUSION

We conclude our study on osteosarcoma detection through the lens of deep learning and neuron activation visualization. Our findings and insights underscore the potential of deep learning to revolutionize the field of medical image analysis, offering both accurate classification and enhanced interpretability. With a multiclass classification accuracy of 88.57%, our approach demonstrates its ability to contribute to more accurate and efficient osteosarcoma diagnosis. The exceptional binary classification accuracy rates of 98%, 96.15%, and 91.89% reaffirm the model's proficiency in distinguishing between critical categories, providing medical practitioners with valuable insights. By highlighting regions

of importance, this visualization aids medical professionals in understanding how the model identifies significant features in histological images, enhancing trust and facilitating collaboration between AI systems and human experts. As we move forward, we envision further refinement of our methodologies and potential extensions of our study. The combination of accurate classification and interpretability offers a promising avenue for enhancing osteosarcoma diagnosis.

7.REFERENCES

[1] H. A. Aziz, M.S. Shamsuddin, and A. H. G. Rigit, "Application of artificial neural networks in predicting scour depth around bridge piers," Neural Networks, vol. 22, no. 8, pp. 1234-1240, Oct. 2009.

[2] A. C. Walls et al., "Structure, Function, and Antigenicity of the SARS-CoV-2 Spike Glycoprotein," Cell, vol. 181, no. 2, pp. 281-292.e6, Apr. 2020.

[3] P. P. Lin, S. Patel, Osteosarcoma, in: Bone Sarcoma, Springer, 2013, pp. 75-97.

[4] L. Kager et al., "Osteosarcoma in Very Young Children," Cancer, vol. 116, pp. 5316-5324, 2010.

[5J. B. Hayden and B. H. Hoang, "Osteosarcoma: basic science and clinical implications," Orthopedic Clinics of North America, vol. 37, pp. 1-7, 2006.

[6] K. Munir, H. Elahi, A. Ayub, F. Frezza and A. Rizzi, "cancers cancer diagnosis using deep learning: A bibliographic review", *Cancers*, vol. 11, Aug 2019.

[7] Z. Li, S. M. R. Soroushmehr, Y. Hua, M. Mao, Y. Qiu, and K. Najarian, "Classifying osteosarcoma patients using machine learning approaches", *2017 39th Annual International Conference of the IEEE Engineering in Medicine and Biology Society (EMBC)*, pp. 82-85, 2017.

[8] K. Simonyan, A. Zisserman, Very deep convolutional networks for large-scale image recognition, arXiv preprint arXiv:1409.1556 (2014).

[9] R. Mishra, O. Daescu, P. Leavey, D. Rakheja and A. Sengupta, Histopathological diagnosis for viable and non-viable tumor prediction for osteosarcoma using convolutional neural network, pp. 12-23, May 2017

[10] E. Jabason, M. O. Ahmad and M. N. S. Swamy, "Hybrid feature fusion using rnn and pre-trained cnn for classification of alzheimer's disease (poster)", *2019 22nd International Conference on Information Fusion (FUSION)*, pp. 1-4, 2019.

[11] Anisuzzaman, D. M., Barzekar, H., Tong, L., Luo, J., and Yu, Z. "A deep learning study on osteosarcoma detection from histological images." *Biomedical Signal Processing and Control*, vol. 69, p. 102931, 2021.

[12] W. Rawat, Z. Wang, Deep convolutional neural networks for image classification: A comprehensive review, Neural computation 29 (2017) 2352–2449.

[13] S. Wang, D. M. Yang, R. Rong, X. Zhan, G. Xiao, Pathology image analysis using segmentation deep learning algorithms, The American journal of pathology 189 (2019) 1686–1698.

[14] A. Serag, A. Ion-Margineanu, H. Qureshi, R. McMillan, M.-J. Saint Martin, J. Diamond, P. O'Reilly, P. Hamilton, Translational ai and deep learning in diagnostic pathology, Frontiers in Medicine 6 (2019).

[15] J. de Matos, A. d. S. Britto, L. E. Oliveira, A. L. Koerich, Double transfer learning for breast cancer histopathologic image classification, in: 2019 International Joint Conference on Neural Networks (IJCNN), IEEE, 2019, pp. 1–8.

[16] H. B. Arunachalam, R. Mishra, O. Daescu, K. Cederberg, D. Rakheja, A. Sengupta, D. Leonard, R. Hallac, P. Leavey, Viable and necrotic tumor assessment from whole slide images of

osteosarcoma using machine-learning and deep-learning models, PloS one 14 (2019) e0210706.

[17] E. Deniz, A. S¸eng¨ur, Z. Kadiro˘glu, Y. Guo, V. Bajaj, U. Budak, Transfer learning based ¨ histopathologic image classification for breast cancer detection, Health information science and systems 6 (2018) 18..
[18] S. J. Pan, Q. Yang, A survey on transfer learning, IEEE Transactions on knowledge and data engineering 22 (2009) 1345–1359.

[19] C. Sun, A. Xu, D. Liu, Z. Xiong, F. Zhao, W. Ding, Deep learning-based classification of liver cancer histopathology images using only global labels, IEEE Journal of Biomedical and Health Informatics 24 (2020) 1643–1651. doi:10.1109/JBHI.2019.2949837.
[20] N. Wahab, A. Khan, Y. S. Lee, Transfer learning based deep cnn for segmentation and detection of mitoses in breast cancer histopathological images, Microscopy 68 (2019) 216–233.
[21] M. Yanagawa, H. Niioka, A. Hata, N. Kikuchi, O. Honda, H. Kurakami, E. Morii, M. Noguchi, Y. Watanabe, J. Miyake, et al., Application of deep learning (3-dimensional convolutional neural network) for the prediction of pathological invasiveness in lung adenocarcinoma: A preliminary study, Medicine 98 (2019).
[22] Y. Celik, M. Talo, O. Yildirim, M. Karabatak, U. R. Acharya, Automated invasive ductal carcinoma detection based using deep transfer learning with whole-slide images, Pattern Recognition Letters (2020)

5. CONTRIBUTION

	Rasel Mahmud	**Sajjad Hossain Shakib**	**Md. Nafiul Islam Nayeem**	**Md. Farhan Ul Asif**	**Contribution (%)**
	20-43867-2	*20-43842-2*	*20-43678-2*	*20-43522-1*	
Conceptualization	70%	10%	10%	10%	100 %
Data curation	100%	0%	0%	0%	100 %
Formal analysis	25%	25%	25%	25%	100 %
Investigation	40%	20%	20%	20%	100 %
Methodology	60%	20%	10%	10%	100 %
Implementation	70%	30%	0%	0%	100 %
Validation	90%	10%	0%	0%	100 %
Theoretical derivations	25%	25%	25%	25%	100 %
Preparation of figures	60%	40%	0%	0%	100 %
Writing – original draft	30%	30%	20%	20%	100 %
Writing – review & editing	35%	25%	20%	20%	100 %